Magnetic Resonance Imaging 59 (2019) 61–67

Contents lists available at ScienceDirect

Magnetic Resonance Imaging

journal homepage: www.elsevier.com/locate/mri

Effect of labelling plane angulation and position on labelling efficiency and cerebral blood flow quantification in pseudo-continuous arterial spin labelling

Magdalena Sokolska[a,*], Alan Bainbridge[a], Alvaro Rojas-Villabona[b], Xavier Golay[b], David L. Thomas[b,c]

[a] Medical Physics and Biomedical Engineering, UCLH Foundation Trust, London, UK
[b] Neuroradiological Academic Unit, Department of Brain Repair and Rehabilitation, UCL Queen Square Institute of Neurology, University College London, 8-11 Queen Square, London, UK
[c] Leonard Wolfson Experimental Neurology Centre, UCL Queen Square Institute of Neurology, Queen Square, London, UK

ARTICLE INFO

Keywords:
Arterial spin labelling (ASL)
Pseudo-continuous ASL (pCASL)
Labelling efficiency
Perfusion
Cerebral blood flow (CBF)

ABSTRACT

Pseudo-continuous arterial spin labelling (pCASL) is the MRI method of choice for non-invasive perfusion measurement in research and clinical practice. Knowledge of the labelling efficiency, α, is essential for accurate quantification of cerebral blood flow (CBF). Typically, a theoretical α value is used, based on an idealistic model and an assumption of spins flowing perpendicularly to the labelling plane. The aim of this work was to investigate the effect of violating this assumption, and to characterize the influence of labelling plane angulation with respect to the vessel direction on labelling efficiency and measured CBF.

The effect of labelling plane angulation on labelling efficiency was demonstrated using a numerical simulation of spins at different velocities. Acquisitions from healthy volunteers were used to test the effect of a range of angulation offsets. Additional sub-optimal positions of the labelling plane with respect to the vertebral arteries, at locations where the direction of flow changes significantly from the head-foot direction, were also considered.

No significant change in the measured CBF was seen when the labelling plane was angled up to 60° to the labelled vessel or when it was placed in sub-optimal positions. This study shows that in adult subjects, the efficiency of pCASL is robust to the angulation and positioning of the labelling plane beyond the range of potential operator error.

1. Introduction

Arterial spin labelling (ASL) enables non-invasive mapping of cerebral blood flow (CBF) and has become an established investigative method in both research and clinical practice [1]. Most early applications of ASL used a pulsed ASL (PASL) labelling scheme, due to the simplicity of its implementation and low power deposition [2,3]. In addition, PASL provides high labelling efficiency, which is robust with respect to vascular anatomy and arterial flow rates. However, a recent consensus paper on ASL [4] has recommended using pseudo-continuous arterial spin labelling (pCASL) [5] rather than PASL, due to the intrinsically higher signal-to-noise ratio of the pCASL perfusion-weighted images. As a result, pCASL is currently considered the method of choice for non-invasive perfusion imaging using MRI.

Quantification of CBF using pCASL requires knowledge of the labelling efficiency, α. Standard practice is to use a single value of α based on Bloch equation simulations of blood water spins travelling perpendicularly to the labelling plane [5,6]. However, factors such as placement of the labelling plane can reduce α and result in incorrect CBF quantification which, in turn, might mislead the diagnosis. Previous studies have investigated the effect of position of the labelling plane in relation to imaging volume [7], or anatomical landmarks [8], and a method of direct labelling efficiency measurement has also been proposed [9]. However, the angulation of the labelling plane with respect to the arterial vessels and its effect on labelling efficiency and CBF quantification has not been studied.

abbreviations: ASL, arterial spin labelling; CBF, cerebral blood flow; pCASL, pseudo-continuous arterial spin labelling; α, labelling efficiency; ICA, internal carotid artery; VA, vertebral artery

* Corresponding author at: Medical Physics and Biomedical Engineering, UCLH Foundation Trust, 235 Euston Road, London NW1 2BU, UK.
E-mail address: Magdalena.Sokolska@nhs.net (M. Sokolska).

https://doi.org/10.1016/j.mri.2019.02.007
Received 22 November 2018; Received in revised form 2 February 2019; Accepted 14 February 2019

Sub-optimal angulation might result from pCASL implementation restrictions, e.g. if the labelling plane angle is fixed to that of imaging volume, or can occur in the vertebral arteries if the labelling plane position and angulation are chosen by primarily considering the anatomy of the internal carotid arteries. This also often arises in elderly patient populations, where it might be impossible to plan the labelling plane perpendicular to all feeding arterial vessels simultaneously due to anatomical variations and age/pathology related changes. In addition, the presence of two ‘ kinks' in segment V3 of the vertebral arteries, close to where the labelling plane is usually placed, may also lead to reduced labelling efficiencies and consequential incorrect CBF quantification. Understanding the sensitivity of pCASL to the position and angulation of the labelling plane with respect to the direction of the arterial vessels will improve reliability and build confidence amongst radiologists requesting and radiographers performing this technique.

In this work we investigated the quantitative effect of imperfect labelling plane angulation and position that might arise in clinical practice with respect to both internal carotid and vertebral arteries on α using simulations and *in vivo* acquisitions. We used a simple model of the angulation effect on α, in which the effective velocity of blood water spins is a function of the angle the vessel makes to the normal of the labelling plane. To evaluate the validity of this approximation, α was simulated using a Bloch equation simulator. *In vivo* measurements were performed and assessed against predicted values. As a proof of principle and to achieve an effect larger than the test-retest variability of pCASL CBF, the labelling train flip angle was reduced in a subset of acquisitions. A ‘ worst-case-scenario’ in which the labelling plane is placed exactly parallel to the vertebral vessels was also considered.

2. Materials and methods

2.1. Theory

In ASL, α is defined as the normalized maximum difference in longitudinal magnetization of the blood between the control and label conditions [10]:

$$\alpha = \frac{M_{z,C} - M_{z,L}}{2M_0} \quad (1)$$

where $M_{z,C}$ and $M_{z,L}$ are the longitudinal magnetizations of arterial blood immediately after passing through the control and labelling planes respectively, and M_0 is the fully relaxed magnetization. For perfect inversion after labelling ($M_{z,L} = -M_0$) together with completely unperturbed magnetization after control ($M_{z,C} = M_0$), $\alpha = 1$.

In pCASL, the inversion of flowing spins is realized by using a long train of short RF pulses and field gradients [5]. The amplitude of the RF pulses and the mean field gradient are chosen to ensure best inversion for spin velocities in the relevant range (e.g. 20–38 cm/s, based on the velocity of blood in supplying arteries with the highest flow contribution through the cardiac cycle [11]). Since the normal to the labelling plane designates the direction of the pCASL gradients, any deviation of the vessel orientation from the normal results in the component of the spin velocity along the gradient direction, υ_{eff}, being reduced:

$$\upsilon_{eff}(\xi) = |\upsilon| \cos \xi \quad (2)$$

where υ is the spin velocity and ξ is the angle the vessel makes with respect to the normal of the labelling plane (Fig. 1 a–b). This reduction in spin velocity along the gradient direction may consequently reduce the labelling efficiency.

2.2. Simulations

To estimate the theoretical labelling efficiency, a Bloch equation simulator was implemented in Matlab (The Mathworks Inc., Natick, MA 2016), similar to that described previously [6]. Spins were simulated over a flow distance of 20 cm with a laminar cross-sectional flow profile and maximum flow velocity was varied in the range 1 to 100 cm/s, with a step size of 1 cm/s. The pCASL gradients (gradient during RF pulse, G_{max} = 6 mT/m; average gradient, G_{ave} = 0.6 mT/m) and RF pulse train (Hanning shaped RF pulses of 0.5 ms duration, 1 ms spacing, flip angle (FA) =18°) were matched to the standard vendor ‘balanced’ [6] implementation on a Philips Achieva 3T scanner. The effective labelling plane angulation ξ was set to 0° and 30°, to represent ideal placement and a maximum likely error made by an operator in a typical acquisition, respectively. Additionally, pCASL pulse trains were simulated as above but with ξ at the more extreme value of 60°, and also with FA = 8° for ξ = 0° and 60°. While 60° does not represent angulation or FA = 8° a pulse train likely to occur in practice for a pCASL acquisition, it serves as a ‘ proof of principle’ case which is expected to show significant differences compared to the standard pulse train, and thus help to provide validation of the simulation predictions. T_1/T_2 of the arterial blood were assumed to be 1.65 s/0.165 s [4,12].

2.3. Imaging protocol

Eight healthy volunteers (4 females, mean/SD age 28/3 years) underwent scans after providing written consent. Imaging was performed on a 3T Philips Achieva (Philips Healthcare, Best, The Netherlands), using a 32 channel head coil and the standard pCASL vendor implementation (software version R3.1, unless indicated otherwise). The core protocol included: (i) phase contrast vessel survey; (ii) T1-weighted MPRAGE (TI= 812 ms, TR/TE=6.8/3.1 ms, TFE factor=230, FOV=200× 200×180 mm, spatial resolution=1× 1×1 mm, SENSE acceleration factor=2); (iii) phase contrast quantitative flow scan (PC QFlow,VENC = 60 cm/s, non-gated with 20 averages - flow velocities averaged over cardiac cycle); and (iv) pCASL (labelling duration=1.65 s, post labelling delay=1.8 s, GE-EPI readout: FOV=240× 240 mm, acquisition matrix=64×64 TR/TE=4000/ 15 ms, background and fat suppression enabled, 20 slices). Proton density weighted images with identical readout as pCASL, but with TR= 9 s and no background suppression, were also acquired for CBF quantification. PC and proton density images were acquired three times, distributed in time approximately equally during the scanning session.

The experimental protocol consisted of two parts. In the first part, performed in all volunteers, the pCASL labelling plane was carefully positioned using the vessel survey, centred on the right internal carotid artery, between the carotid bifurcation and the lower ‘kink’ on the vertebral artery (*i.e.* inferior to V3). The angulation (ξ) of the labelling plane to the vessels was set to either 0°, 30° (Fig. 1c) or 60° (Fig. 1d). Acquisitions with each of these configurations were performed twice with 20 repetitions (20 control-label pairs) with the order of acquisition being randomized for each volunteer. The second part of the protocol aimed to investigate the agreement of simulation predictions for reduced FA and the consequences of ‘ worst case scenario’ position, along vertebral arteries (ξ = 90°). Therefore, volunteers were split into two groups for which the protocol consisted of either (i) two scans with reduced flip angle of the labelling train (FA = 8°) and two labelling plane angles ξ = 0° and 60° (4 volunteers) or (ii) additional scans with the standard FA = 18° but with the labelling plane positioned parallel to the flow direction at two locations on the vertebral artery: upper and lower V3 ‘kinks' (Fig. 1e and f, respectively).

3. Post processing

Data were motion corrected by registering all raw images to a volunteer template (the mean image acquired with FA = 18° and ξ = 0°) using DTI-TK [13] software. Each dataset was then pairwise subtracted, averaged (all acquired repetitions for given ξ and FA) and CBF maps were calculated according to the general kinetic model given by Eq. 1 in the ISMRM ASL consensus paper [4]. Cortical voxels were defined for further analysis using FSL [14] FAST binary segmentation [15] and restricting to the right hemisphere only. Internal carotid artery (ICA)

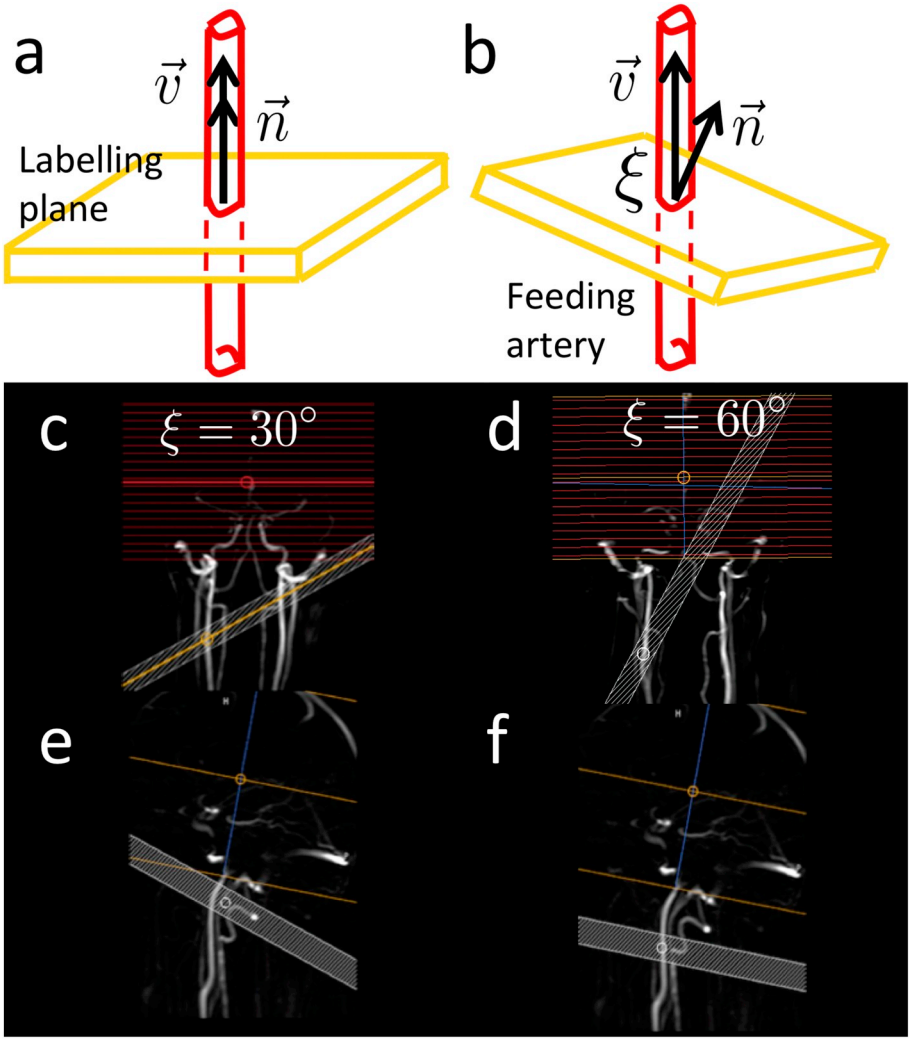

Fig. 1. Theoretical (a,b) and practical (c–f) orientations of the labelling plane. Spins travelling though the labelling plane within an artery perpendicular to the labelling plane (a) and in one that makes an angle with the normal to the labelling plane (b). The position of the labelling plane on a vessel survey for $\xi = 30^{\circ}$ (c), 60° (d) and parallel to the vertebral arteries: V3 'top kink' (e) and V3 'bottom kink' (f).

and vertebral artery (VA) territories were further segmented manually using ITK-SNAP [16]. Watershed regions were avoided when defining the vascular territories. Mean velocities in supplying vessels at the level of the labelling plane were estimated by drawing ROIs on each acquired PC scan and then averaging the calculated values per subject. An example of the segmentation of the feeding arteries for velocity measurement, as well as the segmentation into right cortex and ICA/VA territories, is shown in Fig. 2.

3.1. Relative efficiency estimation

The effect of labelling plane angulation on α was estimated relative to the standard labelling train with perfect angulation (when the labelling plane is perpendicular to the flow direction). For each combination of labelling plane angulation and pCASL flip angle (ξ,*FA*) a relative labelling efficiency was calculated as the ratio of the simulated labelling efficiency for the ξ and *FA* pair, $\alpha_{\xi,FA}$ and that of $\xi = 0^{\circ}$ and $FA = 18^{\circ}$:

$$\alpha_{rel,SIM}(\xi, FA) = \frac{\alpha(\xi, FA)}{\alpha(0^{\circ}, 18^{\circ})} \quad (3)$$

For *in vivo* data, relative efficiency was calculated as the ratio between measured CBF values:

$$\alpha_{rel,MEAS}(\xi, FA) = \frac{CBF(\xi, FA)}{CBF(0^{\circ}, 18^{\circ})} \quad (4)$$

Since α is simply a scaling factor, this approach aimed to remove other variables in CBF quantification. Additionally, the maximum blood velocities measured from QFlow scans in the right ICA and VA were used as input parameters to simulate the relative labelling efficiencies for a given velocity.

3.2. Statistical analysis

A single factor ANOVA was used to test for differences in the mean CBF values when acquisition conditions were varied. Three groups of tests were performed: (i) constant $FA = 18^{\circ}$ and three different angulations ($\xi = 0^{\circ}$,30° and 60°) in each ROI; (ii) constant $FA = 18^{\circ}$ and three different positions on VA in the VA ROI; (iii) constant $FA = 8^{\circ}$ and $\xi = 0^{\circ}$ and 60° together with $FA = 18^{\circ}$ and $\xi = 0^{\circ}$ in each ROI. A pairwise t-test was used to investigate differences in cases where statistically significant difference between groups was determined by ANOVA. An F-test was used to test for differences in the variance of the signal in each ROI with each labelling plane orientation. A p-value < 0.05 was considered statistically significant.

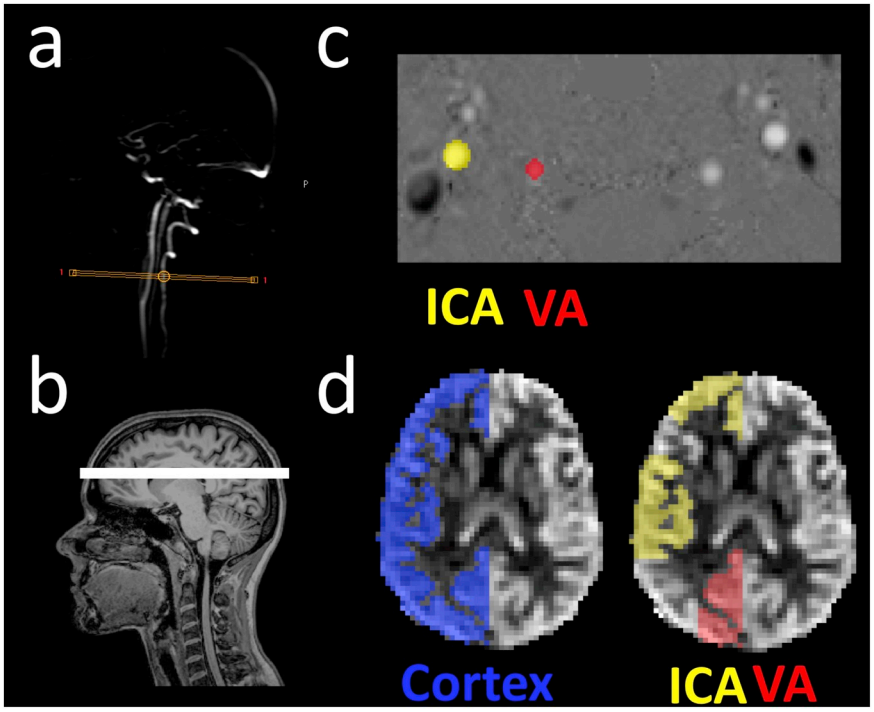

Fig. 2. Slice position of PC QFlow (a) and segmentation of feeding arteries for velocity measurement (c). Example segmentation of voxels within cortex, internal carotid artery and vertebral artery (d) for a single slice (b).

4. Results

Fig. 3 shows the simulated labelling efficiency as a function of the flow velocity in the vessel for different combinations of ξ and FA. Overall, for the pulse trains studied, the inversion process is remarkably robust to the angle between the vessel and the normal to the labelling plane. For the highest velocities, labelling efficiency increases with ξ. The simulations suggest that for blood velocities above $\sim$ 53 cm /s, $\xi = 60^{\circ}$ should show greater labelling efficiency than $\xi = 0^{\circ}$ for the standard labelling train $FA = 18^{\circ}$; when the labelling train $FA = 8^{\circ}$, this velocity threshold reduces to $\sim$ 16 cm /s.

Fig. 4 shows $\alpha_{rel,SIM}$ and $\alpha_{rel,MEAS}$ plotted against the maximum velocity measured *in vivo* in the internal carotid and vertebral arteries. In Fig. 4a $\alpha_{rel,SIM}$ was estimated using the Bloch Equation simulations and Eq. (3); in Fig. 4b, $\alpha_{rel,MEAS}$ was computed from mean regional CBF values and Eq. (4). In the range of measured velocities, simulated $\alpha_{rel,SIM}$ (Fig. 4a) for $\xi = 30^{\circ}$ is very similar to that of $\xi = 30^{\circ}$ ($\alpha_{rel,SIM} \sim 1$, range from 0.98 to 1.01) and slightly higher than when $\xi = 60^{\circ}$ ($\alpha_{rel,SIM} < 1$, range 0.89 –0.98) for pCASL $FA = 18^{\circ}$. However, for $FA = 8^{\circ}$, $\alpha_{rel,SIM}$ is higher for $\xi = 60^{\circ}$ (range 0.73 –0.83) than $\xi = 0^{\circ}$

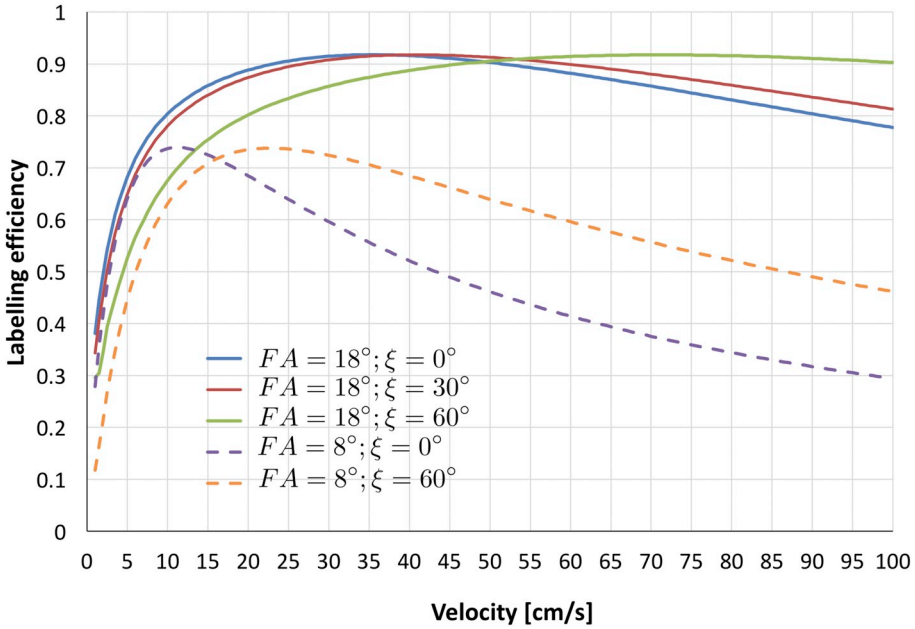

Fig. 3. Simulated efficiency for different and flip angles for a range of velocities. Labelling plane was set at $\xi = 0^{\circ}$ and T_1 and T_2 were set to 1.65 s and 0.165 s, respectively. Scanner default settings of the pCASL train was used: $G_{max} = 6$ mT/m, $G_{ave} = 0.6$ mT/m, $\Delta = 1$ ms, $\delta = 0.5$ ms.

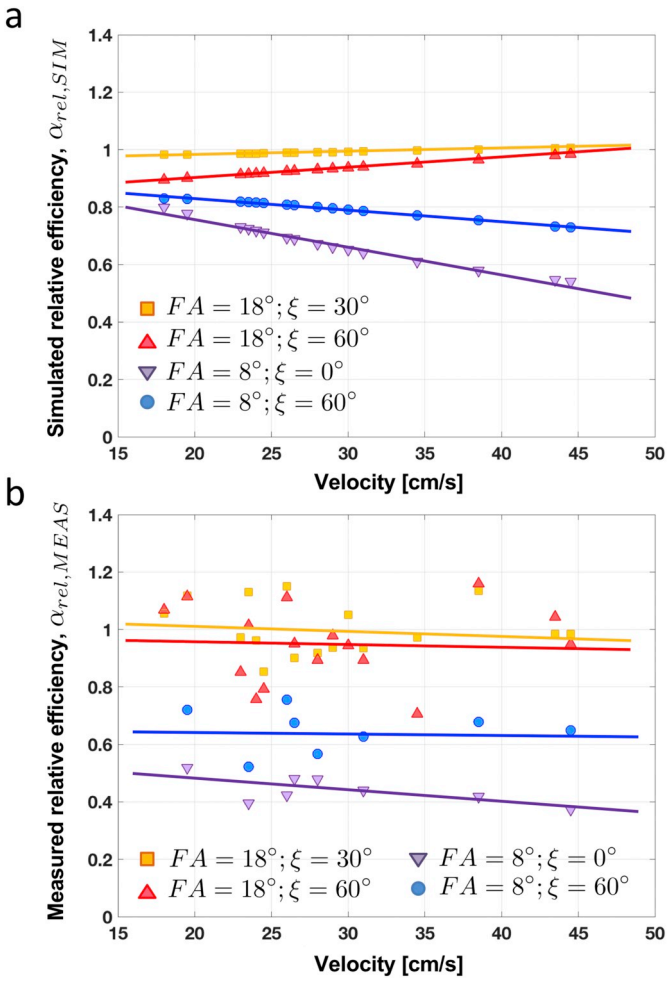

Fig. 4. Relative efficiency as a function of the blood velocity measured *in vivo* in carotid and vertebral arteries. Relative efficiency estimated based on simulations (a) and *in vivo* data (b).

(0.54 –0.80). The same trend can be observed for $\alpha_{rel,MEAS}$ calculated from quantified regional CBF (Fig. 4b) measured *in vivo*.

Fig. 5 shows mean CBF values for all different conditions measured in different territories. There was no statistically significant difference in CBF between group means as determined by one-way ANOVA for (i) $FA = 18°$ with three different angulations ($\xi = 0°$,30° and 60°) or (ii) $FA = 18°$ with three different VA positions ($\xi = 0°$, positioned below the ‘ lower kink’ and at the ‘ upper kink’ and ‘ lower kink’ levels, where the labelling plane is approximately parallel to the blood flow direction *i.e.* theoretically $\xi \sim 90°$) in any of ROIs. However, there was a statistically significant difference between group means for (iii): $FA = 8°$ ($\xi = 0°$ and 60°) and $FA = 18°$ ($\xi = 0°$) in all ROIs ($p < 0.005$). A further investigation with pairwise t-tests revealed a statistical significant difference between each of the pairs compared in (iii) ($p < 0.005$). There were no statistically significant differences in variance of the signal in vertebral artery territory ROI with each labelling plane orientation.

5. Discussion

This study investigates the influence of both the position and the angulation of the pCASL labelling plane, in relation to the anatomy of the brain feeding vessels, on the labelling efficiency in healthy adult subjects. The consensus paper recommends positioning the labelling plane either perpendicular to the vessels or by following other anatomical landmarks [4]. However, if the labelling plane is fixed parallel to the imaging volume, prioritising the labelling plane position to be perpendicular to the vessels may result in sub-optimal FoV angulation. Alternatively, positioning the labelling plane based on the recommended distance of 8.5 cm from the AC-PC line [7] or at the base of the skull [17] could result in large inter-patient variation in the labelling plane angulation and position with respect to the vessel anatomy. More recent work [8] suggests that positioning the labelling plane with respect to anatomical landmarks (between C2 and C3 cervical vertebrae or above the carotid artery bifurcation and below the V3 segment of the vertebral arteries) is beneficial and avoids the ‘ kinks' of the V3 segment. However, in an elderly population, and in patients with torturous vessels or vascular disease, this might still result in a sub-optimal angle, the effect of which has not previously been studied.

The deviations from ideal perpendicular labelling plane angulations in this work are modelled by reduction of the spin velocity. The results of simulations for this model of efficiency dependence on angulation show only very small $\alpha_{rel,SIM}$ differences for $\xi = 30°$ and some efficiency reduction for $\xi = 60°$ up to blood velocities of 50 cm/s, but still within a test-retest error of CBF measurement with pCASL of 20% [18]. This can be explained by the fact that the proportional reduction in velocity will be 13% and 50% respectively at these two angles. Much larger, measurable, reduction of relative efficiency can be observed when the *FA* of the labelling train is reduced to 8°, with $\alpha_{rel,SIM}$ of $\xi = 60°$ higher than that of $\xi = 0°$ or 30° (Fig. 4a). These observations are confirmed *in vivo* for the measured range of velocities (15–50 cm/s) and therefore this proof of concept experiment confirms the validity of the presented angulation model assumptions. However, the quantitative agreement between the modelled $\alpha_{rel,SIM}$ and the measured $\alpha_{rel,MEAS}$ is poorer for $FA = 8°$ than for $FA = 18°$. This may be due to the lower SNR of the measured CBF caused by a lower labelling efficiency affecting the $\alpha_{rel,MEAS}$ measurement accuracy.

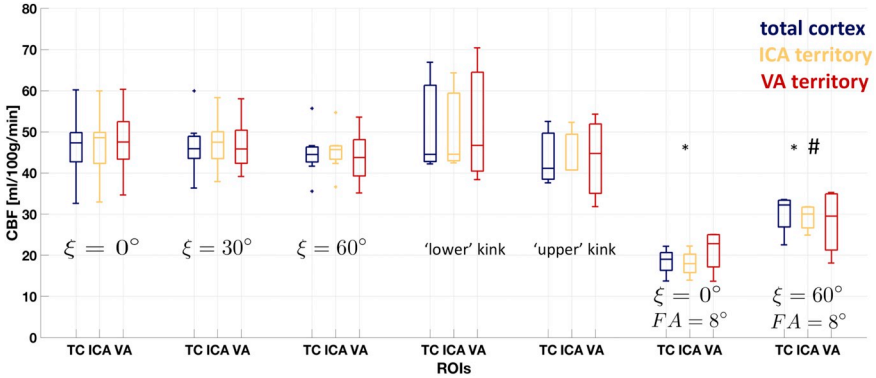

Fig. 5. CBF values for different ROIs and acquisitions, averaged for all volunteers. The boxes represent the 25th and 75th percentile, the line across is the median and whiskers are the spread of the data. * t-test $p < 0.05$ when compared to $FA = 18°$, $\xi = 0°$, # t-test $p < 0.05$ when compared to $FA = 8°$, $\xi = 0°$.

An equivalent approach to simulate the influence of the labelling plane angulation, rather than reduction of velocity, would be to reduce the G_{max}/G_{ave} gradients to 5.2 /0.52 mT/m or 3 / 0.3 mT/m for $\xi = 30^{\circ}$ and $\xi = 60^{\circ}$ respectively. However, the advantage of velocity reduction approach is that it is conceptually simpler and allows prediction of the behaviour of the efficiency vs velocity curve without additional simulations.

In vivo measurements show no statistically significant differences between CBF for 3 different angulation angles, which implies high robustness of pCASL to angulation of the labelling plane. Also, there were no statistically significant differences between CBF when the plane was positioned at the V3 'kink' points on the vertebral arteries, compared to the ideal location. This is initially surprising, as it suggests that the labelling plane angulation can be taken up to 90°. This would result in zero velocity through the gradient and a lack of flow driven inversion, if the labelling plane were infinitively thin. However, inversion of the blood water protons clearly still occurs. This happens for two reasons: (i) the finite thickness of the labelling plane and (ii) perturbation of magnetisation vector during the transit through the kink. Firstly, the labelling plane thickness (~ 13 mm for the RF pulse/gradient combination used in this work) is much greater than a vessel diameter. Therefore, some spin inversion occurs during the approach to and exit from the straight part of the ' kink'. Secondly, the blood water experiences excitation pulses while traveling along the direction of the labelling plane, which affects the magnetisation vector. The relative degree of these two effects depends on the time the blood takes to move through the ' kink', which in turn depends on blood velocity as well as ' kink's' length. The spread of the data and standard deviation in the VA territory is the highest for the ' lower kink' labelling position. Although not statistically significant (F-test $p > 0.05$), possibly due to a small group size, this suggests that careful positioning on the vertebral arteries is more important than on carotid arteries. The standard deviation is also elevated in the ICA territory when the labelling plane is positioned on the ' kinks'. This is most likely a result of a large anatomical variation of the vertebral vessels between subjects resulting in similar variation of the angle of the labelling plane to the ICA. Further, the variable distance, and therefore transit time, between the labelling plane and the brain tissue in the imaging plane will also contribute to the increased standard deviation.

Interestingly, labelling efficiency increases with ξ for high flow velocities, which can be present in certain pathologies, such as sickle cell anaemia. However, if the velocity of the flow is known a priori in high flow cases, a correct (lower) labelling efficiency should be used in the final CBF calculation, or alternatively, the labelling train appropriately adapted.

High robustness of the pCASL labelling train to labelling plane angulation observed in this study results from the approximately flat shape of efficiency vs velocity curve in the broad region of velocities. Therefore, even for large angulations, which result in significant reduction of effective velocity, pCASL still provides good labelling efficiency.

5.1. Limitations

One limitation of this study is the low sample size and recruitment restricted to young, healthy volunteers. However, the study was intended as a proof of principle investigation, and even from this limited number of volunteer data sets, it is clear that predictions of the simulations match well with the *in vivo* results.

The effect of tilting the labelling plane was modelled as an effective reduction of the spin velocity. This simple model was used to illustrate the effect when considering straight vessels with constant velocity of flow. However, if the vessel tortuosity is such that blood flow effectively descends around the V3 segment of the vertebral arteries, as can occur in elderly persons, then the model is less able to describe the net effect of a tilted labelling plane. In such a scenario, more complex simulations would be required.

Another study limitation is the use of manual ROI identification, assuming standard territories of ICAs and VAs. Although less common, non-standard configurations of the Circle of Willis (CoW) could have been present in our volunteers (for example, a fetal origin of the PCA) which would influence the regional findings. While time of flight angiograms were not acquired as part of our protocol due to time limitations, the results of the regional analysis follow the predictions made by simulations based on the measured velocities. Therefore, we conclude that non-standard CoW configurations did not contribute to the results.

The exact prediction of the effect of labelling plane angulation on ξ are specific to the design of the pCASL gradient and pulse train, which in turn is specific to a vendor or implementation. However, the shape of curve of the efficiency change with velocity is similar for all designs, and therefore the presented results are likely to be valid in general, especially for the small range of labelling plane orientation angles more likely found in day-to-day practice.

6. Conclusions

In summary, this study shows that in healthy adult subjects, the efficiency of pCASL using a standard, vendor-implemented labelling pulse train is highly robust to angulation of the labelling plane and feasible angulation errors are unlikely to contribute to CBF quantification errors.

Funding

This work was undertaken at UCLH/UCL, which received a proportion of funding from the Department of Health's NIHR Biomedical Research Centres funding scheme. DLT is supported by the UCL Leonard Wolfson Experimental Neurology Centre (PR/ylr/18575).

References

[1] Haller S, Zaharchuk G, Thomas D L, Lovblad K-O, Barkhof F, Golay X. Arterial spin labeling perfusion of the brain: emerging clinical applications. Radiology 2016;281(2):337–56. https://doi.org/10.1148/radiol.2016150789.

[2] Edelman R R, Siewert B, Darby D G, Thangaraj V, Nobre A C, Mesulam M M, et al. Qualitative mapping of cerebral blood flow and functional localization with echo-planar MR imaging and signal targeting with alternating radio frequency. Radiology 1994;192(2):513–20. https://doi.org/10.1148/radiology.192.2.8029425.

[3] Petersen E T, Zimine I, Ho Y C, Golay X. Non-invasive measurement of perfusion: a critical review of arterial spin labelling techniques. Br J Radiol 2006;79(944):688–701. https://doi.org/10.1259/bjr/67705974.

[4] Alsop D C, Detre J A, Golay X, Günther M, Hendrikse J, Hernandez-Garcia L, et al. Recommended implementation of arterial spin-labeled Perfusion mri for clinical applications: a consensus of the ISMRM Perfusion Study group and the European consortium for ASL in dementia. Magn Reson Med 2015;73(1):102–16. https://doi.org/10.1002/mrm.25197.

[5] Dai W, Garcia D, De Bazelaire C, Alsop D C. Continuous flow-driven inversion for arterial spin labeling using pulsed radio frequency and gradient fields. Magn Reson Med 2008;60(6):1488–97. https://doi.org/10.1002/mrm.21790.

[6] Wu W C, Fernández-Seara M, Detre J A, Wehrli F W, Wang J. A theoretical and experimental investigation of the tagging efficiency of pseudocontinuous arterial spin labeling. Magn Reson Med 2007;58(5):1020–7. https://doi.org/10.1002/mrm.21403.

[7] Aslan S, Xu F, Wang P L, Uh J, Yezhuvath U S, Van Osch M, et al. Estimation of labeling efficiency in pseudocontinuous arterial spin labeling. Magn Reson Med 2010;63(3):765–71. https://doi.org/10.1002/mrm.22245.

[8] Zhao L, Vidorreta M, Soman S, Detre J A, Alsop D C. Improving the robustness of pseudo-continuous arterial spin labeling to off-resonance and pulsatile flow velocity. Magn Reson Med 2017;78(4):1342–51. https://doi.org/10.1002/mrm.26513.

[9] Chen Z, Zhang X, Yuan C, Zhao X, van Osch M J. Measuring the labeling efficiency of pseudocontinuous arterial spin labeling. Magn Reson Med 2017;77(5):1841–52. https://doi.org/10.1002/mrm.26266.

[10] Williams D S, Detre J A, Leigh J S, Koretsky A P. Magnetic resonance imaging of perfusion using spin inversion of arterial water. Proc Natl Acad Sci 1992;89(1):212–6. https://doi.org/10.1073/pnas.89.1.212.

[11] Jahanian H, Noll D C, Hernandez-Garcia L. B 0 field inhomogeneity considerations in pseudo-continuous arterial spin labeling (pCASL): effects on tagging efficiency and correction strategy. NMR Biomed 2011;24(10):1202–9. https://doi.org/10.1002/nbm.1675.

[12] Lee T, J a Stainsby, Hong J, Han E, Brittain J, G a Wright. Blood relaxation properties at 3T - effects of blood oxygen saturation. Proc Intl Soc Mag Reson Med 2003;11:131.
[13] Zhang G. http://dti-tk.sourceforge.net/pmwiki/pmwiki.php. (2.3.3).
[14] Jenkinson M, Beckmann C F, Behrens T E, Woolrich M W, Smith S M. FSL. NeuroImage 2012;62(2):782–90. https://doi.org/10.1016/j.neuroimage.2011.09.015.
[15] Zhang Y, Brady M, Smith S. Segmentation of brain MR images through a hidden Markov random field model and the expectation-maximization algorithm. IEEE Trans Med Imaging 2001;20(1):45–57. https://doi.org/10.1109/42.906424.
[16] Yushkevich P A, Piven J, Hazlett C, Smith G, Ho S, Gee J C, et al. User-guided 3D active contour segmentation of anatomical structures: significantly improved efficiency and reliability. NeuroImage 2006;31:1116–28. https://doi.org/10.1016/j.neuroimage.2006.01.015.
[17] Dai W, Robson P M, Shankaranarayanan A, Alsop D C. Reduced resolution transit delay prescan for quantitative continuous arterial spin labeling perfusion imaging. Magn Reson Med 2012;67(5):1252–65. https://doi.org/10.1002/mrm.23103.
[18] Gevers S, Van Osch M J, Bokkers R P H, Kies D A, Teeuwisse W M, Majoie C B, et al. Intra- and multicenter reproducibility of pulsed, continuous and pseudo-continuous arterial spin labeling methods for measuring cerebral perfusion. J Cereb Blood Flow Metab 2011;31(8):1706–15. https://doi.org/10.1038/jcbfm.2011.10.